Kramers problem in periodic potentials: Jump rate and jump lengths

R. Ferrando, R. Spadacini, and G. E. Tommei

*Dipartimento di Fisica dell'Università di Genova, Centro di Fisica delle Superfici e delle Basse Temperature
del Consiglio Nazionale delle Ricerche, via Dodecaneso 33, 16146, Genova, Italy*
(Received 25 May 1993)

The Kramers problem in periodic potentials is solved separating the intrawell and interwell dynamics. Both the jump rate and the probability distribution of the jump lengths are obtained by a Fourier analysis of the decay function $f(q)$; at high and intermediate potential barriers, in the first Brillouin zone, $f(q)$ essentially coincides with the energy half-width of the quasielastic peak of the dynamic structure factor. The method is applied to the Klein-Kramers dynamics; numerical results are obtained in a wide damping range by solving the Klein-Kramers equation with cosine potential and homogeneous friction, at high $(16k_B T)$ and intermediate $(6k_B T)$ potential barriers. The jump rate exhibits the expected turnover behavior; an increasing deviation from the exponential decay of the jump-length distribution is found as the damping decreases. The low-friction, multiple-jump regime is quantitatively characterized. The comparison with asymptotic analytical approximations of the Mel'nikov and Meshkov kind suggests that finite-barrier corrections are significant even at high potential barriers, especially in the underdamped regime.

PACS number(s): 05.40.+j, 82.20.Db, 05.20.Dd, 05.60.+w

I. INTRODUCTION

The theory of noise-activated transitions among states of local stability is a topic of great importance in many areas [1]. In particular, a large class of phenomena in physics and chemical physics may be modeled on the basis of the Brownian motion in an external potential U; in that case the proper transport equation is a Fokker-Planck equation (FPE) with an external force [2,3]. The first solution to the escape problem of a classical particle, subjected to a thermal Gaussian white noise, out of a deep potential well was obtained by Kramers [4]. He calculated the escape rate r in the two opposite limits of high and very low friction η (spatial and energy diffusion, respectively); in both cases Kramers results are asymptotic and become exact in the limit of a very high energy barrier E_a. Kramers turnover theory was originally developed for a metastable well with only one escape path, in order to elucidate some points in reaction-rate theory. Due to the relevance of his contribution the escape-rate problem is now commonly known as the Kramers problem [5,6] and the corresponding FPE is called the Klein-Kramers equation (KKE) [2].

Substantial improvements of the Kramers theory have been obtained only in the last decade. Several authors [7–9] found corrections to the linear dependence of r on η in the underdamped limit, obtaining a reasonable behavior in the turnover region, not covered by the Kramers formulas. Recently, memory effects [5,10–15], position-dependent friction [16,17], and finite-barrier corrections, both in the spatial-diffusion regime [18–20] and at low friction [5,21] have also attracted considerable attention.

The largest part of the results on the Kramers problem concerns the metastable [5,6] and bistable [5,9,22] potentials, which are of primary interest in the study of chemi-

cal kinetics. In condensed-matter physics we find a variety of phenomena, ranging from superionic conduction [23] and atom diffusion at crystal surfaces [24] to Josephson-junction theory [2,6], which may be conveniently described by the KKE with a periodic (or tilted periodic) potential. Particularly rich is the phenomenology in the field of surface diffusion of classical adatoms. In this case the surface periodic potential originates from the underlying crystal and is in general a temperature-dependent free energy [25,26]; thus, in high-temperature diffusion, the barrier height may be of the same order of magnitude as the thermal energy $k_B T$ [24,27] and then far from the asymptotic Kramers limit. Moreover, also the friction in the plane parallel to the surface may depend periodically on the adatom position, being stronger at the well bottoms than at the saddle points [25].

The Kramers problem in a periodic potential [28] is qualitatively different from the escape problem out of a metastable well mainly for two reasons.

First, the periodic potential is multistable and the escaped particle may be again trapped, due to the presence of the thermal fluctuations, in any other well; this means that jumps of a single lattice spacing or of many lattice spacings are possible [29]. In the following, jumps longer than a single lattice spacing will be referred to as "multiple jumps" and the escape rate r_j in a periodic potential will be called the jump rate. The full solution of the Kramers problem in periodic potentials must include the calculation of the jump-length probability distribution (JLPD) [28]. Evidence of multiple jumps has been recently found in the diffusion of adsorbates at crystal surfaces, both experimentally [30] and in molecular dynamics simulations [31]. Activation of multiple jumps is clear evidence of low-friction diffusion [29].

Second, in the periodic case there are two equivalent escape paths (to the left and to the right side) instead of

the single path of the metastable well. The relationship between the total jump rate r_j from a periodic well and the escape rate r from a likewise metastable well is not trivial. It results that $r \leq r_j \leq 2r$ as the friction increases from zero to infinity [28,32]; in fact, while in the spatial-diffusion regime the flux of escaping particles is controlled by the number of escape paths, at very low friction all the particles with energy greater than the barrier energy can escape independently of their position in the well and of the direction of their velocity.

Up to now, the diffusion in a periodic potential has been studied mainly from the point of view of the calculation of the diffusion coefficient D and of some correlation functions such as the velocity autocorrelation spectrum and the mean-square displacement [2,33–35,29]. At high barriers, in the jump-diffusion regime, D is simply related to r_j and to the mean-square jump length $\langle l^2 \rangle$ [35]:

$$D = \tfrac{1}{2} r_j \langle l^2 \rangle \ . \tag{1.1}$$

The separation of r_j and $\langle l^2 \rangle$ allows a detailed description of the diffusive motion; in general, this separation is not trivial except for the case of high friction, where only single jumps are possible and $\langle l^2 \rangle = a^2$, with a the lattice spacing.

In spite of the great interest in diffusion problems in lattice systems and of the relevant advances in the study of the Fokker-Planck dynamics [2,29], the results for the Kramers problem in periodic potentials are few [5]. Here we can mention an old (and of debated paternity [36]) exact calculation of the diffusion coefficient D [37,38] in the very-high-friction limit, where the dynamics is well accounted for by the simple Smoluchowski equation (SE) [2,3,5,39] and r_j is simply related to D by Eq. (1.1) [40,35], because the diffusion proceeds by single jumps [29]. Recently Mel'nikov presented in his review paper [6] an approximate formula for the r_j and the JLPD in a periodic (really the more general tilted periodic) potential. In a different context Moro and Polimeno [41] solved the Kramers problem in a fourfold periodic potential with cyclic boundary conditions. They were able to calculate numerically the partial transition rates to different wells; however, due to the cyclic boundary conditions, they could not distinguish jumps which differ by a multiple of four lattice spacings (for instance, they could not distinguish between a triple jump to the left and a single jump to the right).

In this paper we will develop the theoretical approach sketched in a previous Rapid Communication [28]; the Kramers problem will be exactly (this term will be more precisely defined in the following) solved for a one-dimensional periodic potential $U(x)$ (without tilt), calculating both the jump rate r_j and the JLPD. The method can be applied to any kind of periodic potentials and also to position-dependent friction; in this paper it will be applied to the case of a cosine potential with homogeneous friction. Other shapes of $U(x)$ and a position-dependent friction will be treated in a forthcoming paper. The jump rate r_j and the JLPD will be obtained by comparing two expressions for the dynamic structure factor S_s. The first expression is derived from jump-diffusion theory and it

contains r_j and the jump-length probabilities as parameters; the other is obtained by numerically solving the KKE with the matrix-continued-fraction method (MCFM) [2,29]. The numerical results for r_j and for the JLPD will be compared with analytical approximations of the Mel'nikov and Meshkov kind [6,9,32].

The starting point of any rate theory is a clearcut separation of time scales, the rate itself being a well-defined quantity only if the escape events are rare [5,6]. This fact may be expressed in different ways as a weak-noise limit [5] or as a metastability condition [6]. In both cases the inverse rate is requested to be much larger than a typical time scale of the well dynamics, such as the period of the small oscillations at the well bottom τ_{osc}. In periodic systems the rate problem has a precise sense if the intrawell dynamics is faster than the interwell dynamics, characterized by τ_{th}, i.e., by the time employed to cross a unit lattice spacing by a particle traveling at the thermal equilibrium velocity. Therefore the rate condition, $\tau_{\text{osc}} \ll \tau_{\text{th}}$, is essentially a jump condition [29] and implies $E_a \gg k_B T$; actually the exponential dependence of the rate on E_a allows a precise definition of r_j as E_a is of few $k_B T$ ($E_a \geq 5 k_B T$ in the case of a cosine potential [6,29,42]). The important point is that the Kramers problem in a periodic potential is a kind of refined jump theory where the entering parameters (r_j and jump probabilities) are fully specified by the underlying kinetic equation, not necessarily a FPE: in fact the jump rate problem has been solved with the same method also in the case of the linearized Boltzmann equation with the Bhatnagar-Gross-Krook (BGK) collision kernel [43]. In the usual jump theory [44] r_j and the JLPD are phenomenological parameters, often estimated by employing the transition-state-theory rate r_{TST} and neglecting the possibility of multiple jumps; this approach can lead to large errors both in the overdamped and in the underdamped regime [31,45].

Although multiple jumps seem to play an important role in surface diffusion [30,31] and in chemical-physics problems [41], results about the JLPD are very few, the most important being the approximate analytical solution by Mel'nikov [6]; the phenomenological assumption of an exponential decay of the jump probabilities [46] is not fully supported by the Fokker-Planck dynamics, in particular at low friction where the initial energy distribution of the escaping particles deviates strongly from the equilibrium distribution [9,47]. A precise separation of the low-friction multiple-jump regime from the single-jump regime is still lacking [29].

The paper is organized as follows. In Sec. II the theory is fully developed in the general case. In Sec. III the numerical results about r_j and the JLPD are presented and compared to analytical approximations for the case of cosine potential and homogeneous friction. Both high ($E_a = 16 k_B T$) and low ($E_a = 6 k_B T$) barriers are treated in detail. The conclusions are contained in Sec. IV.

II. THEORY

As stated in the Introduction, the jump rate r_j and the JLPD are calculated by comparing two expressions for

the dynamic structure factor. The first expression is derived from jump-diffusion theory and contains r_j and the jump probabilities as parameters; the other expression is obtained by numerically solving the Klein-Kramers equation with the MCFM.

Consider a particle diffusing in a periodic potential $U(x)$ with minima in the positions $\ldots, -a, 0, a, \ldots$. The particle is coupled to a heat bath by a friction η, which, in the general case, may depend on the position x; the time evolution of its phase-space probability distribution $f(x, v, t)$ is ruled by the KKE

$$\frac{\partial f}{\partial t} = -v \frac{\partial f}{\partial x} - \frac{F(x)}{m} \frac{\partial f}{\partial v} + \eta(x) \frac{\partial}{\partial v} \left[vf + \frac{k_B T}{m} \frac{\partial f}{\partial v} \right] ,$$

(2.1)

where $F(x) = -U'(x)$. The dynamic structure factor $S_s(q, \omega)$ is the time Fourier transform of the characteristic function $\Sigma_s(q, t)$:

$$S_s(q, \omega) = \frac{1}{2\pi} \int_{-\infty}^{\infty} \Sigma_s(q, t) e^{-i\omega t} dt ,$$

(2.2)

with

$$\Sigma_s(q, t) = \langle \exp\{iq[x(t) - x(0)]\} \rangle ,$$

(2.3)

where the angle brackets refer to the thermal average. Σ_s can be calculated from the probability density $f(x, v, t)$ solving the proper kinetic equation [29,43], in our case the KKE (2.1).

Let us consider the motion of the particle from the point of view of jump-diffusion theory, in order to get one of the above-mentioned expressions of the dynamic structure factor. In order to separate the intracell and intercell dynamics, we can split the quantity $x(t)$ in two parts:

$$x(t) = al(t) + x_c(t) ,$$

(2.4)

where the cell index $l(t)$ is integer and $-a/2 < x_c(t) < a/2$. The same splitting is done for $x(0)$; therefore Σ_s is written as

$$\Sigma_s(q, t) = \langle \exp\{iqa[l(t) - l(0)]\} \exp\{iq[x_c(t) - x_c(0)]\} \rangle .$$

(2.5)

If the dynamics inside a cell and the diffusive motion among the lattice sites are characterized by well-separated time scales, as happens in the case of sufficiently high barriers, the right-hand side in Eq. (2.5) can be factorized as

$$\Sigma_s(q, t) = \langle \exp\{iqa[l(t) - l(0)]\} \rangle$$
$$\times \langle \exp\{iq[x_c(t) - x_c(0)]\} \rangle .$$

(2.6)

At times much larger than $1/\eta_w$, where η_w is the value of the friction at the bottom of the potential wells, the second factor in Eq. (2.6) relaxes to a function of q only and Σ_s becomes of the form

$$\Sigma_s(q, t) = h(q) \Sigma_s^D(q, t) ,$$

(2.7)

with

$$\Sigma_s^D(q, t) = \langle \exp\{iqa[l(t) - l(0)]\} \rangle .$$

(2.8)

Σ_s^D describes the motion among the sites of the discretized lattice and can be obtained by solving a proper master equation for the probability $P(la, t)$ of finding the diffusing particle in the lth cell at a certain time t. The particle hops out of the cell with a rate r_j and can thermalize in any other cell; the probability of thermalizing in the cell around $(l + n)a$, with $n \neq 0$, is π_n. Notice that r_j is the total jump rate; the partial rate for a jump to the cell in $(l + n)a$ is given by the quantity $r_j \pi_n$. The evolution of $P(la, t)$ is described by

$$\frac{dP(la, t)}{dt} = r_j \sum_{n(\neq 0)} \pi_n \{ P[(l + n)a, t] - P(la, t) \} .$$

(2.9)

This master equation is solved with the condition of having the particle in the lth cell at the time 0. In an even system the probability of jumps of equal length to the right or to the left are equal,

$$\pi_{-n} = \pi_n ;$$

(2.10)

therefore, having introduced the probability P_n of a jump of length $|n|a$

$$P_n = \pi_n + \pi_{-n} ,$$

(2.11)

the following expression for Σ_s^D is obtained:

$$\Sigma_s^D(q, t) = \exp[-f(q)t] ,$$

(2.12)

where $f(q)$ is an even periodic function of q which contains the jump rate and the jump-length probabilities as parameters:

$$f(q) = r_j \sum_{n=1}^{\infty} P_n [1 - \cos(naq)] .$$

(2.13)

Finally, from Eqs. (2.2), (2.7), and (2.12) we get an expression for the dynamic structure factor S_s, which results in a simple Lorentzian form:

$$S_s(q, \omega) = \frac{h(q)}{\pi} \frac{f(q)}{f^2(q) + \omega^2} .$$

(2.14)

Equation (2.14) has been obtained by making a factorization [see Eq. (2.6)] and a relaxation approximation [see Eq. (2.7)]. Therefore we expect S_s, as given by the solution of the proper kinetic equation, to be of the form (2.14), with $f(q)$ periodic, if both q and ω are sufficiently small. In particular we expect the form (2.14) to give a good description of the quasielastic peak of S_s as a function of ω at fixed q; the inelastic peaks, which are related to the well dynamics and may appear in S_s at ω multiple of the small-oscillation frequency $\omega_{\rm osc}$ [48,29], are obviously not described by Eq. (2.14). Moreover we expect Eq. (2.14) to improve its validity at large amplitudes of the potential, because in this case the diffusive dynamics and the well dynamics are characterized by very different time scales. We will check the approximations leading to Eq. (2.14) for the specific example discussed in the following section. A third approximation has been made by neglecting the time of flight between lattice sites with respect to the inverse jump rate in the master equation

(2.9); this approximation has been discussed in detail in Ref. [42], where it has been shown that its validity improves exponentially with the barrier height. In particular it results that the time of flight is two orders of magnitude shorter than the inverse rate for a cosine potential with a barrier of about $4k_B T$, in the spatially limited diffusion regime.

From Eq. (2.14) $f(q)$ can be extracted as

$$f(q) = \lim_{\omega \to 0} \omega \left[\frac{S_s(q,0)}{S_s(q,\omega)} - 1 \right]^{-1/2} . \tag{2.15}$$

If S_s is exactly a Lorentzian at every ω, the limit in the right-hand side of Eq. (2.15) is not necessary. The Lorentzian shape implies the full width at half maximum (FWHM) $\Delta\omega(q)$ of S_s, which was considered in Refs. [28,43], to be simply $2f(q)$. Of course, in general this is not true, but, as we will see in the following section for a cosine potential, $f(q)$ and $\Delta\omega(q)/2$ tend rapidly to become equal as the potential barrier increases.

The jump rate r_j and the jump-length probabilities are recovered by integrations [28]:

$$r_j = \frac{a}{\pi} \int_0^{\pi/a} f(q) dq , \tag{2.16}$$

$$P_n = -\frac{2a}{\pi r_j} \int_0^{\pi/a} f(q) \cos(naq) dq . \tag{2.17}$$

Now, if we are able to solve in some way the KKE calculating the dynamic structure factor, we can obtain the function $f(q)$ by making the limit specified in Eq. (2.15) [or equivalently from $\Delta\omega(q)/2$] and the jump rate and the JLPD can be obtained by Eqs. (2.16) and (2.17), respectively.

The most efficient numerical method to solve the KKE is the MCFM, developed by Risken (see Ref. [2], where a complete description of the method with many applications is given). In the periodic case the MCFM is based on the expansion of the solution into a basis set of plane waves for the position variable and of Hermite functions for the velocity variable. The method allows the numerical calculation of the Green function of the KKE (i.e., of

the conditional probability distribution), by which the average contained in the definition (2.3) of the characteristic function Σ_s can be computed. The details of the numerical method for the calculation of the dynamic structure factor S_s, in the general case of position-dependent friction, are given in [29]. Here we only report the results. First of all, it is convenient to define some dimensions variables:

$$\bar{x} = \frac{2\pi}{a} x , \quad \bar{F}(\bar{x}) = \frac{a}{2\pi} \frac{F(x)}{k_B T} ,$$

$$\bar{U}(\bar{x}) = \frac{U(x)}{k_B T} , \quad \bar{\gamma}(\bar{x}) = \frac{a}{2\pi} \left[\frac{m}{k_B T} \right]^{1/2} \eta(x) , \tag{2.18}$$

$$\bar{t} = \frac{2\pi}{a} \left[\frac{k_B T}{m} \right]^{1/2} t ;$$

in these units the lattice spacing is 2π and the first Brillouin zone in reciprocal space corresponds to $|q| \leq \frac{1}{2}$. The rate is obviously normalized as an inverse time. In the following we will use these dimensionless quantities, if not otherwise specified. Moreover, for simplicity, we will write these variables without overline.

The expression for the dynamic structure factor results:

$$S_s(q,\omega) = 2N \, \text{Re} \left[\sum_{p,l=-\infty}^{\infty} \tilde{G}_{00}^{pl}(k,i\omega) M_{p-r} M_{l-r}^* \right] ,$$

$$\tag{2.19}$$

where $q = r + k$ with r integer, $-\frac{1}{2} < k \leq \frac{1}{2}$, and

$$M_r = \frac{1}{2\pi} \int_{-\pi}^{\pi} dx \, \exp\left[-\frac{1}{2} U(x) \right] \exp(irx) . \tag{2.20}$$

The coefficients M_r are real in the case of even potentials. The normalization factor N is given by

$$N^{-1} = \int_{-\pi}^{\pi} dx \, \exp[-U(x)] \tag{2.21}$$

and the matrix $\tilde{G}_{00}$ is expressed by a matrix continued fraction:

$$\tilde{G}_{0,0}(k,z) = (z\underline{I} + \underline{B}_+ \{z\underline{I} + \underline{\Gamma} + 2\underline{B}_+ [z\underline{I} + 2\underline{\Gamma} + 3\underline{B}_+ (z\underline{I} + 3\underline{\Gamma} + \cdots)^{-1} \underline{B}_-]^{-1} \underline{B}_- \}^{-1} \underline{B}_-)^{-1} . \tag{2.22}$$

The matrices $\underline{\Gamma}$, $\underline{B}_+$, and $\underline{B}_-$ are given by

$$\Gamma^{lp} = \frac{1}{2\pi} \int_{-\pi}^{\pi} dx \, \exp(-ilx) \gamma(x) \exp(ipx) ,$$

$$iB_+^{lp}(k) = \frac{1}{2\pi} \int_{-\pi}^{\pi} dx \, \exp[-i(l+k)x] B(x)$$
$$\times \exp[i(p+k)x] , \tag{2.23}$$

$$iB_-^{lp}(k) = \frac{1}{2\pi} \int_{-\pi}^{\pi} dx \, \exp[-i(l+k)x] \hat{B}(x)$$
$$\times \exp[i(p+k)x] ,$$

with

$$B(x) = \frac{\partial}{\partial x} + \frac{1}{2} F(x) , \quad \hat{B}(x) = \frac{\partial}{\partial x} - \frac{1}{2} F(x) . \tag{2.24}$$

For practical purposes the matrix continued fraction (2.22) has to be truncated to a certain number of iterations; obviously matrices of finite size must be used. Details about the number of iterations and the size of the matrices needed to achieve a good numerical convergence can be found in the following section.

III. RESULTS FOR COSINE POTENTIAL AND HOMOGENEOUS FRICTION

Throughout this section we will apply the theory described in Sec. II to the case of cosine potential and

homogeneous friction; in unnormalized units

$$U(x) = -A \cos \left[\frac{2\pi x}{a} \right] , \tag{3.1}$$

$$\eta(x) = \eta . \tag{3.2}$$

In this case the solutions of the KKE depend on two dimensionless parameters; a good choice is the couple (γ, g) defined by

$$\gamma = \frac{a}{2\pi} \left[\frac{m}{k_B T} \right]^{1/2} \eta , \quad g = \frac{A}{2k_B T} . \tag{3.3}$$

γ is the normalized friction and g is related to the energy barrier $E_a = 2A$ by

$$E_a = 4 g k_B T . \tag{3.4}$$

The matrices $\underline{\Gamma}$, $\underline{B}_+$, and $\underline{B}_-$ [Eq. (2.23)] take the form

$$\Gamma^{lp} = \delta^{lp} , \tag{3.5}$$

$$B_{lp}^{\pm}(k) = (p+k)\delta^{lp} \pm \tfrac{1}{2} g (\delta^{l,p+1} - \delta^{l,p-1}) . \tag{3.6}$$

The parameter range that can be covered by the MCFM is very wide: problems arise only at extremely low friction $(\gamma < 10^{-3})$ or at very high barriers $(E_a > 20 k_B T)$. The computational effort is different according to the values of the parameters. In fact, both the size of the matrices and the number of iterations needed to get a good numerical convergence in the computation of $S_s(q, \omega)$ depend on q, ω and on the parameters γ and g. The dependence on ω is weak, at least if we consider ω in the quasielastic peak. The dependence of the number of iterations on q is not negligible. In fact, in the first Brillouin zone it is easier to get the convergence at high q (around $\tfrac{1}{2}$) than at small q. For instance, at $q = \tfrac{1}{2}$, $g = 4$, $\gamma = 10$ matrices 31×31 and five iterations are sufficient to compute S_s with a precision better than one part over 10^6; 12 iterations are necessary at $q = 0.01$. However, the most important dependence is on γ and g. Decreasing γ, both the size and the number of iterations increase and the same happens when increasing g. The effect of γ on the matrices' size is important in the region below the turnover in the rate curve $(\gamma < 1)$; at γ higher than the turnover and g smaller than 5 it is easy to get very precise results without cumbersome computations. At $q = 0.01$, $g = 1.5$, $\gamma = 10$ matrices 13×13 and six iterations are needed for a precision better than one part over 10^6; at $\gamma = 1$ we need the same matrices but with 25 iterations and at $\gamma = 0.1$ (which is well below the turnover, as we will see in the following) we need 190 iterations with matrices 41×41. The calculations become rather cumbersome at $\gamma < 10^{-2}$; for instance, at $\gamma = 10^{-3}$ and $g = 1.5$ a precision better than 1% is achieved with matrices 111×111 and 2000 iterations. The same matrices and iterations are sufficient at $g = 4$ and $\gamma = 5 \times 10^{-3}$.

Let us analyze the behavior of $f(q)$ and of $\Delta \omega(q)/2$ for different values of the potential barrier. $f(q)$ has been extracted from the numerical S_s by Eq. (2.15); $\Delta \omega(q)/2$ has been numerically calculated looking for the half-

width at half maximum of the quasielastic peak of S_s. We will see that both $f(q)$ and $\Delta \omega(q)/2$ tend to the same periodic function as g increases. In Fig. 1 the full line represents $f(q)$ for an intermediate value of the friction $(\gamma = 1)$ and for a rather low potential barrier $(g = 0.25$, corresponding to a barrier of $k_B T)$. In this case $f(q)$ is clearly not periodic, as $\Delta \omega(q)/2$ (dash-dotted line), indicating that the dynamics cannot be described, even approximately, by any discretized jump model. Moreover the two functions are largely different at $q > \tfrac{1}{2}$ (i.e., out of the first Brillouin zone). This fact means that the quasielastic peak cannot be described by a simple Lorentzian, even at rather small q; therefore the approximations leading to Eq. (2.14) are not valid. At higher barriers $(g = 1$, see Fig. 2) $f(q)$ and $\Delta \omega(q)/2$ are periodic and practically coincide in the range of q plotted in the figure (the maximum difference being of about 1%); in this case, in which the barrier is of few $k_B T$, the shape of the quasielastic peak is Lorentzian (at least at ω up to its half-width) in a q range extending to several Brillouin zones.

The periodicity of $f(q)$ can be verified at different values of γ (see Fig. 3). At $\gamma = 1$ the shape of $f(q)$ is very close to a simple cosine; from Eq. (2.13) we see that the cosine is related to single-jump diffusion, i.e., to the case in which $P_1 = 1$ and all the other jump probabilities vanish. At lower γ, $f(q)$ is rather different from a cosine; this implies that long jumps are important. These qualitative indications will be quantitatively analyzed in Sec. III B.
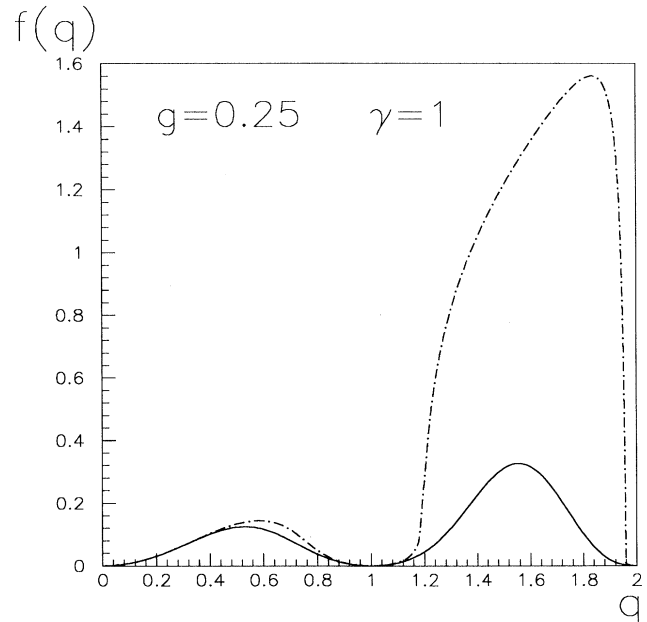

FIG. 1. The function $f(q)$ (full line), defined in Eqs. (2.15), compared with the half-width of the quasielastic peak $\Delta \omega(q)/2$ (dash-dotted line) at a low potential barrier, $E_a = k_B T$, and $\gamma = 1$. The q range in the figure extends to the position of the second diffraction peak.
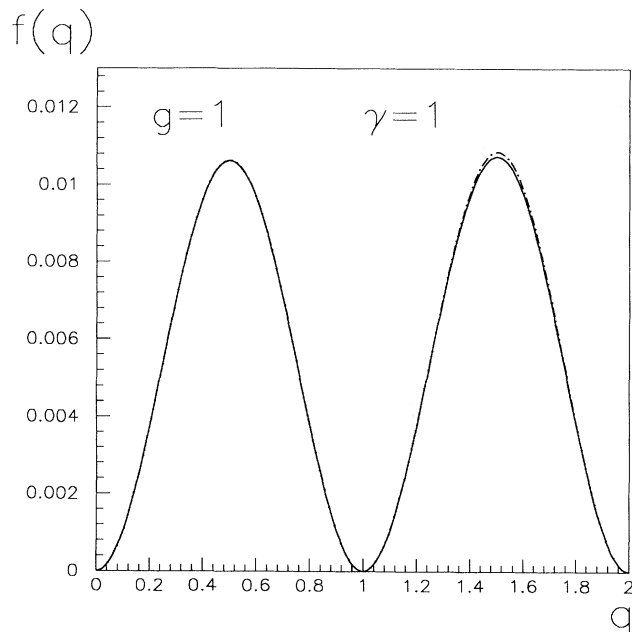
f(q)

FIG. 2. The same as in Fig. 1, but with a barrier of $4k_BT$. The full and the dash-dotted lines almost coincide.
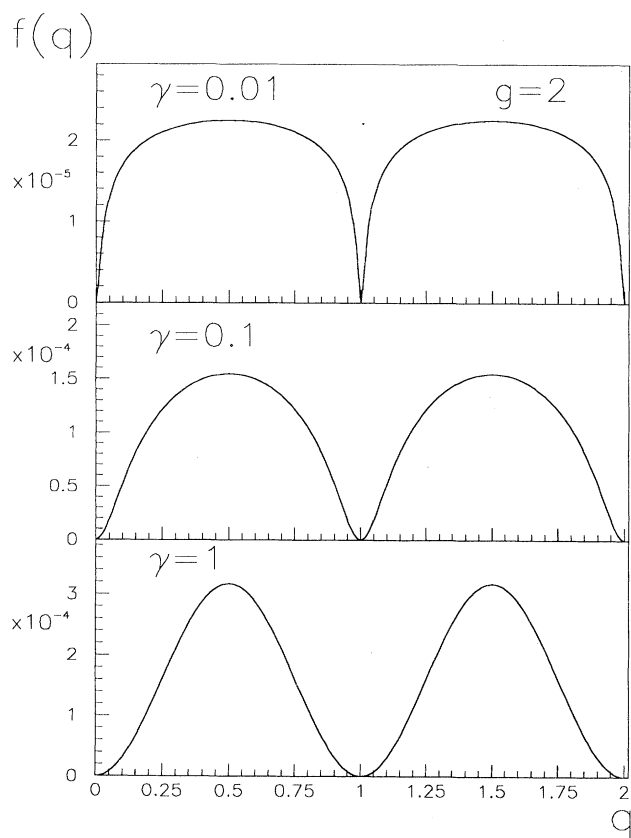
f(q)

FIG. 3. $f(q)$ at a barrier of $8k_BT$ for three different values of the friction.

A. The jump rate r_j

The jump rate r_j is calculated by the numerical integration of $f(q)$, as follows from Eq. (2.16), which, in normalized units, takes the form

$$r_j = 2 \int_0^{1/2} f(q) dq \ . \tag{3.7}$$

In Fig. 4, r_j (full lines) is reported as a function of γ at $E_a = 6k_BT$ and $16k_BT$, respectively. The jump rate r_j exhibits the usual turnover between the low-friction increase and the high-damping $1/\gamma$ behavior. As the barrier increases, the position of the maximum slowly shifts to lower γ values: at $g = 1.5$ the maximum is at $\gamma \simeq 0.56$, at $g = 4$ it is at $\gamma = 0.46$. Moreover, the value of the rate at the maximum, $r_j^{(max)}$, approaches the transition-state rate r_{TST} [49,5],

$$r_{TST} = \frac{\omega_{osc}}{\pi} \exp(-4g) \ , \tag{3.8}$$

where

$$\omega_{osc} = \sqrt{2g} \ . \tag{3.9}$$

In Fig. 4, r_{TST} is represented by the straight dotted lines;

r_j
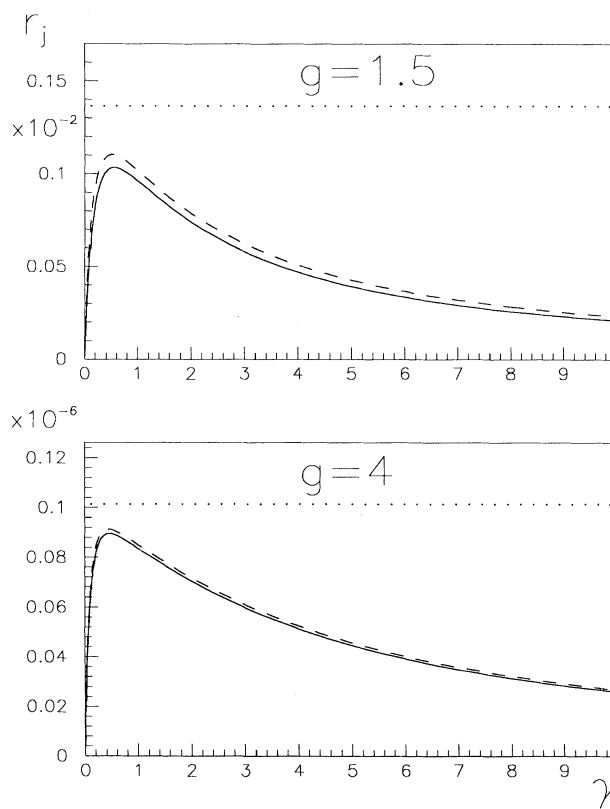
FIG. 4. The jump rate r_j (full lines) as a function of the friction for two different potential barriers $E_a = 6k_BT$ (upper panel) and $E_a = 16k_BT$ (lower panel). The straight dotted lines represent the transition-state rate r_{TST} [see Eq. (3.8)]; the dashed lines are the results for r_M [see Eq. (3.16)].

the difference between r_{TST} and $r_j^{(\text{max})}$ is of about 32% at $g = 1.5$ and of about 13% at $g = 4$.

Of course r_{TST} gives only a rough estimate of the rate in the turnover region; outside this region the numerical results should be compared with more sophisticated theories. An analytical approximation to the jump rate in a periodic potential has been obtained by Mel'nikov [6] by reducing the KKE to an integral equation of Wiener-Hopf type with Gaussian kernel. This approximation, which will be called r_M^{LF} in the following, is valid at low friction, essentially in the region below the turnover. Also r_M^{LF} is expressed by an integral in the first Brillouin zone of a periodic function:

$$r_M^{\text{LF}} = \frac{\omega_{\text{osc}}}{\pi} \exp(-4g) \int_0^{1/2} w(q,\Delta) dq \ , \tag{3.10}$$

the function $w(q,\Delta)$ is given by

$$w(q,\Delta) = 4 \sin^2(\pi q) \exp[2\varphi(q,\Delta) - \varphi(0,2\Delta)] \ , \tag{3.11}$$

with

$$\varphi(q,\Delta) = \sum_{m=1}^{\infty} \frac{1}{m} \text{erfc} \left[\frac{\sqrt{m}\Delta}{2} \right] \cos(2\pi m q) \ . \tag{3.12}$$

The complementary error function $\text{erfc}(x)$ is defined by

$$\text{erfc}(x) = \frac{2}{\sqrt{\pi}} \int_x^{\infty} \exp(-u^2) du \ . \tag{3.13}$$

Δ is the dissipation for a travel from the left to the right at the barrier top; in the case of position-dependent friction [32] Δ is given by

$$\Delta = \frac{1}{k_B T} \int_{-a/2}^{a/2} \eta(x) \sqrt{2m[U_M - U(x)]} dx \ , \tag{3.14}$$

where U_M is the maximum of the potential; for cosine potential and homogeneous friction $U_M = A$ and

$$\Delta = 8\gamma \sqrt{2g} \ . \tag{3.15}$$

An approximation to the jump rate valid in the whole friction range may be obtained by a multiplicative bridging procedure [5,9]. This approximation, which will be referred to as r_M, is given by

$$r_M = \frac{\pi}{\omega_{\text{osc}}} r_M^{\text{LF}} r^{\text{HF}} \exp(4g) \ . \tag{3.16}$$

The high-friction rate r^{HF} is the well-known Kramers formula for spatial diffusion [4], multiplied by a factor 2 because of the two escape paths and generalized in order to take into account the possibility of a position-dependent friction [32]:

$$r^{\text{HF}} = \frac{\omega_{\text{osc}}}{\pi} \left[\left[\frac{\eta_b^2}{4\omega_b^2} + 1 \right]^{1/2} - \frac{\eta_b}{2\omega_b} \right] \exp(-4g) \ , \tag{3.17}$$

where η_b and ω_b are the friction and the curvature at the top of the barriers, respectively; in our case the friction is homogeneous and $\omega_b = \omega_{\text{osc}}$; therefore

$$\frac{\eta_b}{\omega_b} = \frac{\gamma}{\sqrt{2g}} \ . \tag{3.18}$$

It should be noticed that r_M practically coincides with r^{HF} for γ larger than the turnover friction, because, in this limit, the deviations of r_M^{LF} from r_{TST} are exponentially small in Δ [6,9].

The expressions for r_M^{LF} and r^{HF} do not contain finite-barrier corrections and therefore are exact only in the asymptotic limit of high barriers ($g \to \infty$); moreover, they are connected by the bridging expression (3.16), which is clearly an approximation. However, r_M is in very good qualitative agreement with r_j (see Fig. 4); the essential features of the rate curve, such as the position of the maximum, are well reproduced even in the case of rather low barriers. From the quantitative point of view, there are some discrepancies between r_j and r_M; in general r_M overestimates the correct rate. Let us consider the relative difference C between r_M and r_j:

$$C = \frac{r_M - r_j}{r_j} \ , \tag{3.19}$$

which is reported in Fig. 5 as a function of g for three different values of the friction γ. At every γ, as expected, C is a decreasing function of g, r_M being asymptotically correct in the limit of high barriers. In the spatial-diffusion regime ($\gamma = 10$), C is not very large, being less than 0.11 at $g = 1.5$ and less then 3.5×10^{-2} at $g = 4$. In this regime the discrepancies between r_j and r_M have been recently explained [19] by taking into account the finite-barrier corrections to r^{HF}; a very accurate analytical approximation to r_j is obtained by considering the first-order term in the expansion in $1/g$ of those corrections. In the turnover region ($\gamma = 1$), C is even smaller, whereas it becomes larger in the region below the turn-
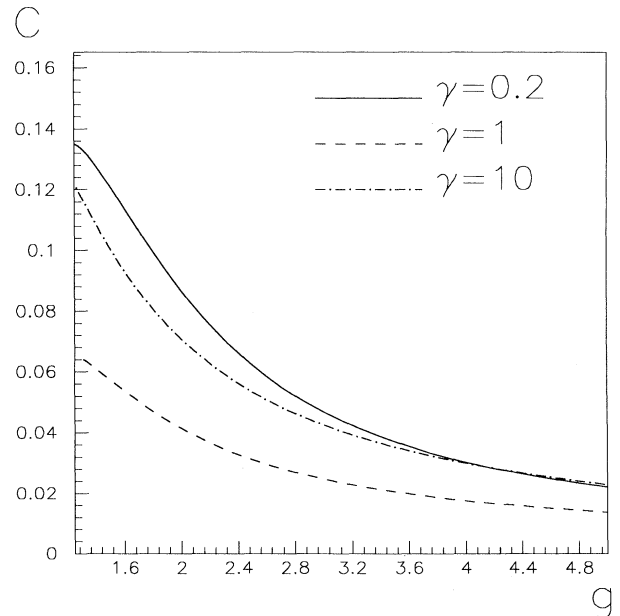

FIG. 5. Relative difference C [see Eq. (3.19)] between r_M [Eq. (3.16)] and r_j as a function of g for three different damping regimes.

over ($\gamma = 0.2$). However, the smallness of C around the turnover may be due to compensation effects introduced by the multiplicative bridging; in the turnover region and below, the discussion of the discrepancies between the numerical results and the analytical approximation is better done by comparing r_j and r_M^{LF}, i.e., by discussing the behavior of the relative difference C^{LF}:

$$C^{LF} = \frac{r_M^{LF} - r_j}{r_j} . \tag{3.20}$$

In Fig. 6 C^{LF} is reported as a function of γ at rather low ($g = 1.5$) and at high ($g = 4$) barriers. It is clearly shown that the relative difference between the numerical results and the analytical approximation becomes more important in the energy-diffusion regime. For instance, C^{LF} is larger than 0.35 at $g = 1.5$ and $\gamma = 10^{-3}$ and larger than 0.1 at $g = 4$ and $\gamma = 5 \times 10^{-3}$. Therefore even at barriers of the order of $20 k_B T$ the difference is not negligible. Also at very low friction the discrepancies between the two results decrease with g and probably they may be explained by taking into account the finite-barrier corrections; however, to our knowledge, there are not analytical calculations of those corrections for a periodic potential in the region below the turnover. It should be pointed out that the magnitude of the finite-barrier corrections at very low friction depends significantly on the shape of the potential, in particular on the shape at the barrier top [5]. For instance, the corrections should be even more important for a potential with a "flat" maximum, such as a potential with vanishing second derivative at the position of the maximum. On the contrary, the corrections should

be less important for a potential with a cusp. However, the cosine potential may represent a large class of potentials of interest in physical problems; different potential shapes will be treated elsewhere [50]. In the region around the turnover and above, C^{LF} increases; this is due to the fact that the approximations leading to r_M^{LF} are not fulfilled; in fact, while the correct rate r_j reaches a maximum and then decreases, r_M^{LF} is monotonically increasing with the friction and tends to r_{TST} [Eq. (3.8)] in the limit $\gamma \to \infty$.

Finally, we remark that in Ref. [28], the jump rate r_j has been compared with an analytical expression, of the Mel'nikov and Meshkov kind, for the escape rate r_{BM} out of a symmetric bimetastable potential. Above the turnover r_M and r_{BM} do not differ at all; below the turnover there are small differences, of the order of a few percent; as could be expected, r_M results in better agreement with r_j, but the whole discussion of the differences between r_j and r_M can be essentially repeated also for the difference between r_j and r_{BM}.

B. The probability distribution of the jump lengths

The jump-length probability distribution is obtained by the Fourier analysis of the function $f(q)$, as follows from Eq. (2.17). In normalized units Eq. (2.17) takes the form

$$P_n = -\frac{4}{r_j} \int_0^{1/2} f(q) \cos(2\pi n q) dq . \tag{3.21}$$

The Wiener-Hopf method furnishes also an analytical approximation to the jump probabilities [6]. In the following the analytically calculated jump probabilities will be called P_n^M. The P_n^M are correspondingly obtained by the
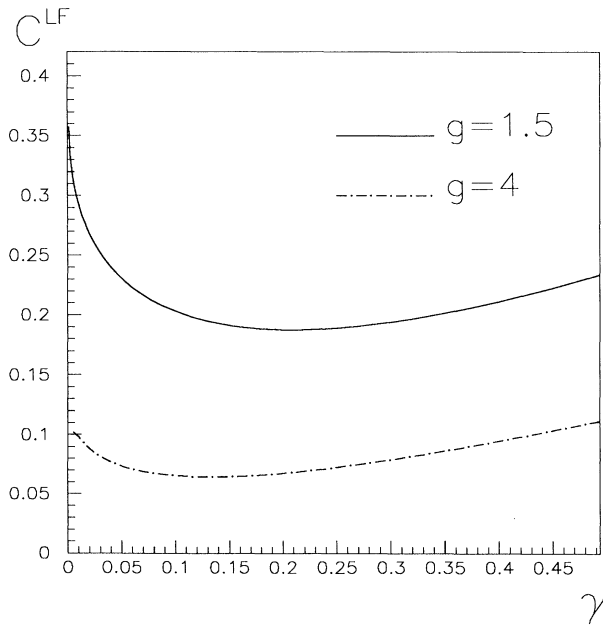

FIG. 6. Relative difference C^{LF} [see Eq. (3.20)] between r_M^{LF} [Eqs. (3.10)–(3.13)] and r_j as a function of γ at low ($g = 1.5$) and high ($g = 4$) potential barriers. The underdamped regime is considered.
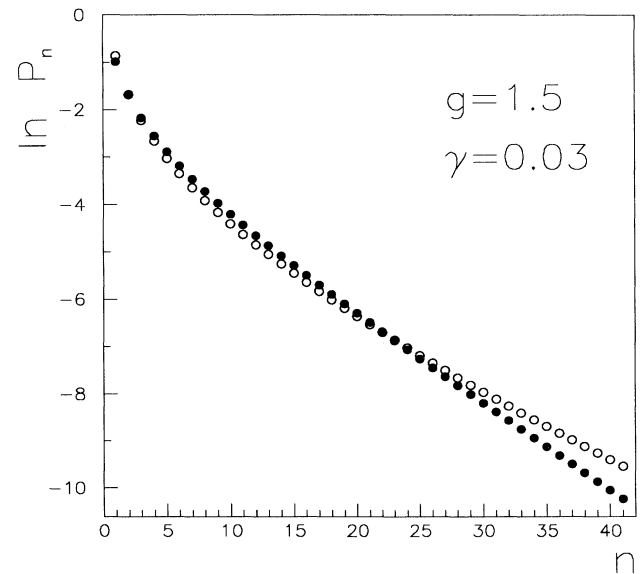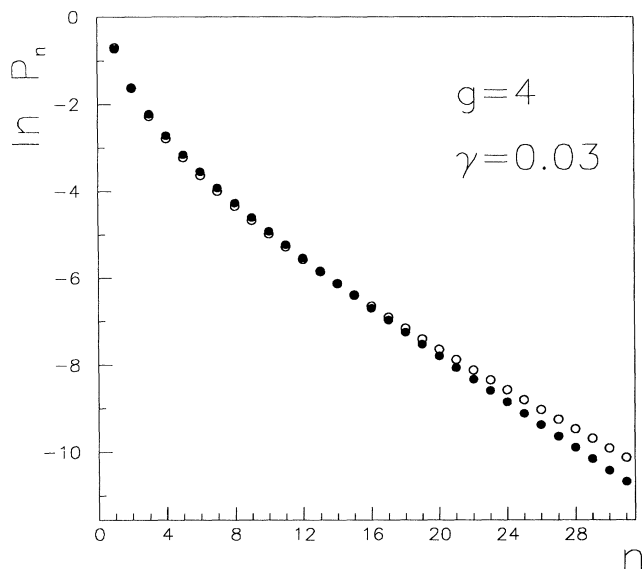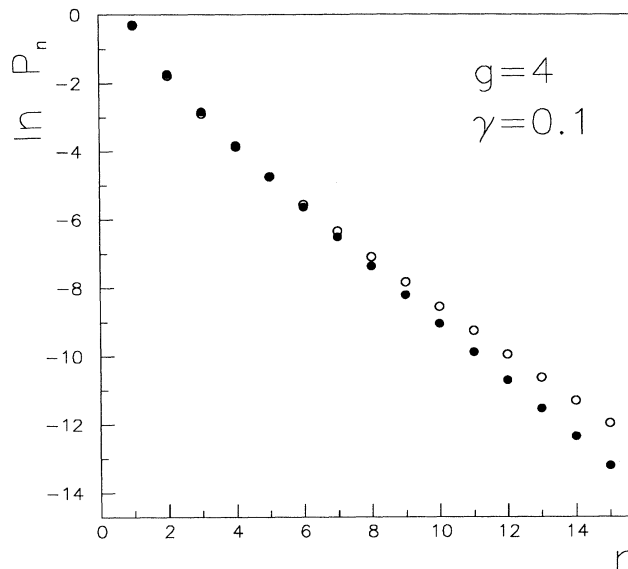

FIG. 7. The jump-length probability distribution (JLPD) at $g = 1.5$ and $\gamma = 0.03$. The black dots correspond to the numerically calculated probabilities P_n [see Eq. (3.21)], the open circles to the analytical approximation P_n^M [see Eq. (3.22)].

FIG. 8. The same as in Fig. 7, but at different γ and g.

FIG. 10. The same as in Fig. 7, but at different γ and g.

Fourier analysis of the function $w(q,\Delta)$, defined in Eq. (3.11);

$$P_n^M = -2\int_0^{1/2} w(q,\Delta)\cos(2\pi nq)dq \left[\int_0^{1/2} w(q,\Delta)dq\right]^{-1}.$$

(3.22)

The results on the JLPD are reported in Figs. 7–21. In Figs. 7–10 the behavior of $\ln(P_n)$ (black dots) and of the analytical approximation (open circles) is reported up to rather high n, in order to study also the asymptotic behavior of the probabilities. Four couples (γ,g) are selected in the region below the turnover, where multiple

jumps become important, as will be clear in the following. The important parameter which determines the decay of the P_n is the dissipation Δ; as expected, long-jump probabilities decrease as Δ increases. In any case, the numerical results are consistent with an asymptotic exponential decay of the P_n for large n. However, at $\gamma=0.03$ and for both values of g, deviations from the exponentiality become evident up to rather large n. The decay of short-jump probabilities is faster. The deviations from exponentiality are less important at $\gamma=0.1$.
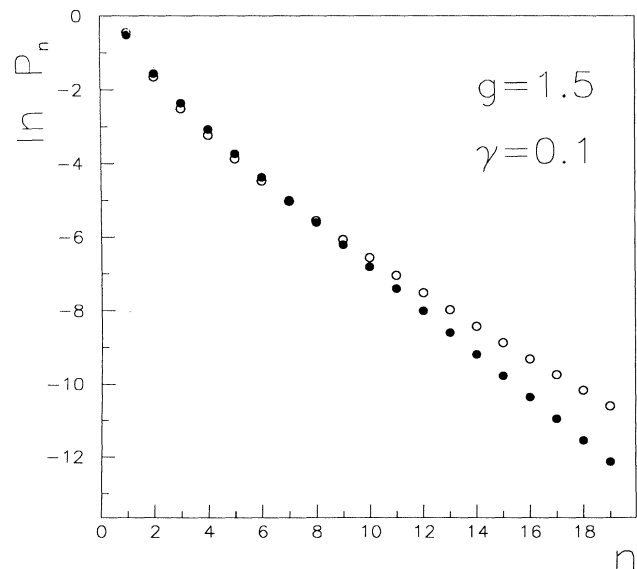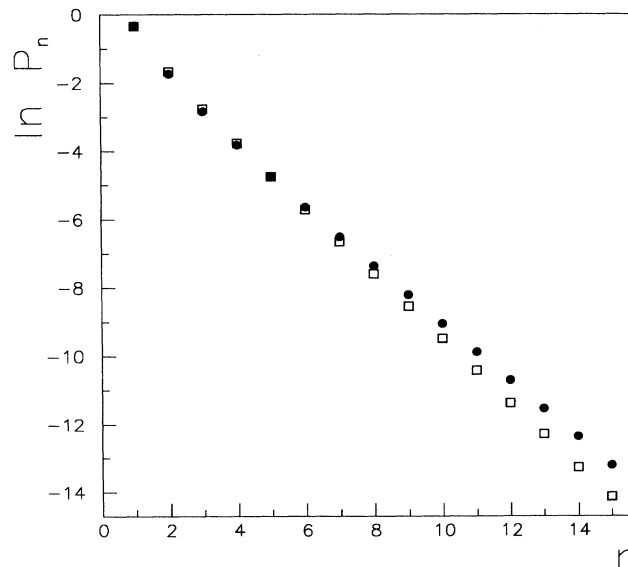

FIG. 9. The same as in Fig. 7, but at different γ and g.

FIG. 11. The JLPD for two different couples (γ,g) corresponding to the same dissipation Δ [see Eq. (3.15)]. Black dots: $\gamma=\frac{1}{10}$, $g=4$. Squares: $\gamma=(\frac{2}{75})^{1/2}$, $g=\frac{3}{2}$.
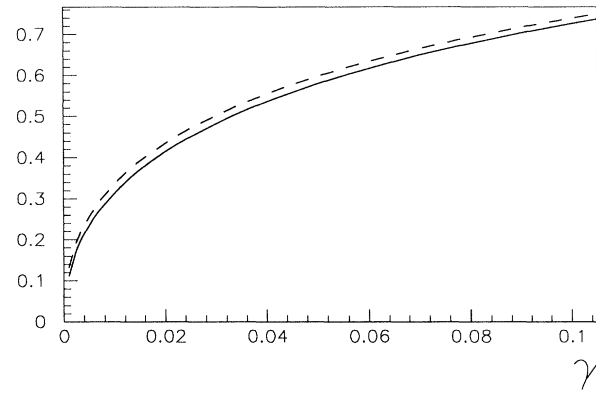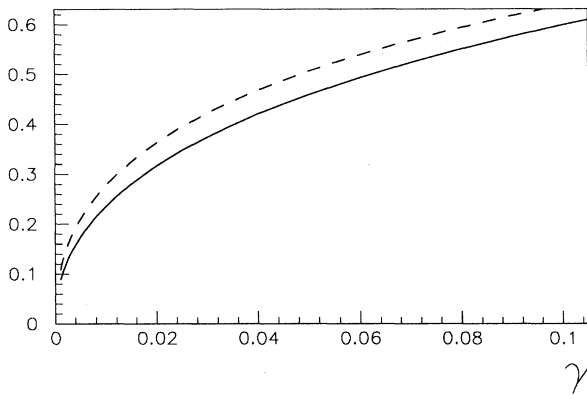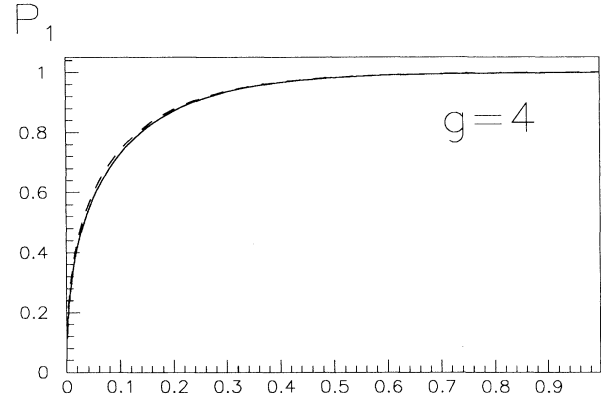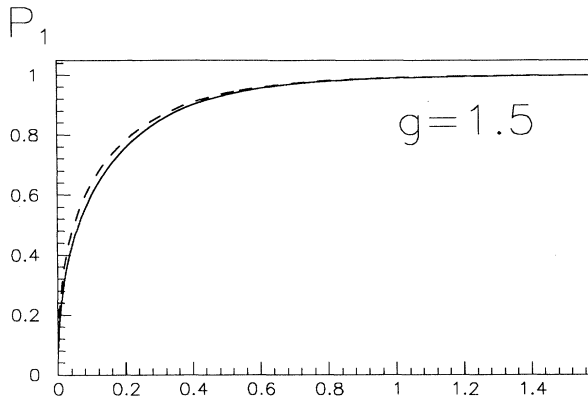
FIG. 12. The single-jump probability P_1 (full lines) as a function of γ at a barrier of $6k_BT$. The dashed lines are the analytical approximation P_1^M [see Eq. (3.22)]. In the lower panel the underdamped regime is magnified.

FIG. 13. The same as in Fig. 12, but at a potential barrier of $16k_BT$.

A qualitative explanation of the behavior of the P_n may be given by considering the energy distribution of the escaping particles out of the cell of departure. At low friction, the energy distribution deviates strongly from the equilibrium Boltzmann distribution [47,9], being shifted to lower energies; the average energy decreases proportionally to $\Delta^{1/2}$ [9]. The particles with less energy are more probably captured in the first wells; after having passed some wells (whose number depends on how strong the deviations from equilibrium in the initial distribution were) most of the low-energy particles have been captured and the distribution of the traveling particles becomes an equilibrium distribution. Beyond this point, the decay of the P_n becomes exponential, as happens in the case of higher friction, where the energy distribution of the escaping particles is already an equilibrium distribution out of the well of departure.

At small n, the analytical approximation (3.22) is in good agreement with the P_n, especially in the case of high g and small dissipation, i.e., at very low friction. In fact, the hypotheses leading to Eq. (3.22) are essentially two [6]: first of all, the energy barrier E_a/k_BT is assumed to be very large; then, the dissipation on the unit cell Δ must be much lower than the energy barrier. Therefore we ex-
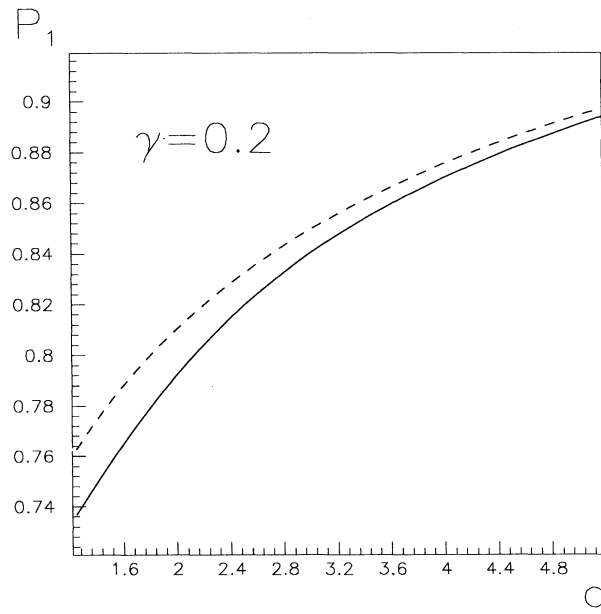

FIG. 14. Single-jump probability P_1 (full lines) as a function of g at a friction $\gamma=0.2$. The dashed line is the analytical approximation P_1^M [see Eq. (3.22)].
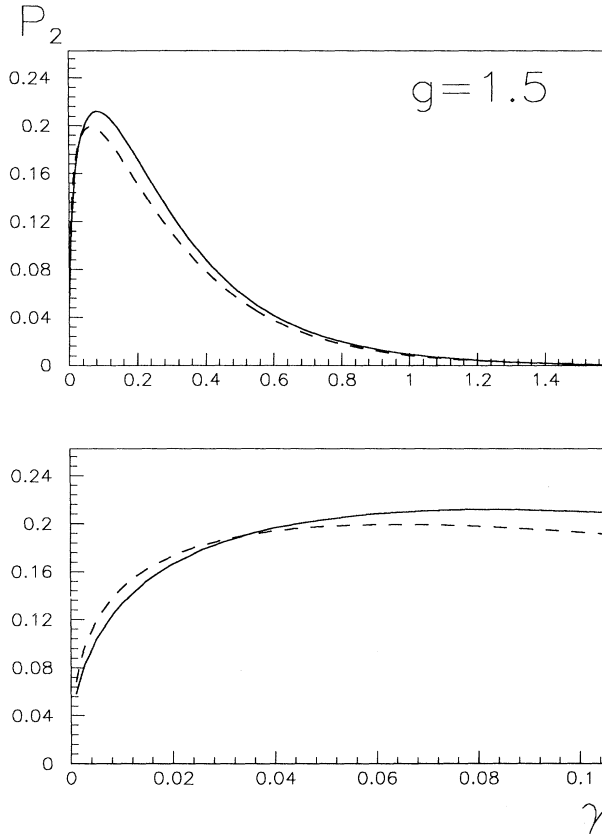
FIG. 15. Double-jump probability P_2 (full lines) as a function of γ at a barrier of $6k_B T$. The dashed lines are the analytical approximation P_2^M [see Eq. (3.22)]. In the lower panel the underdamped regime is magnified.
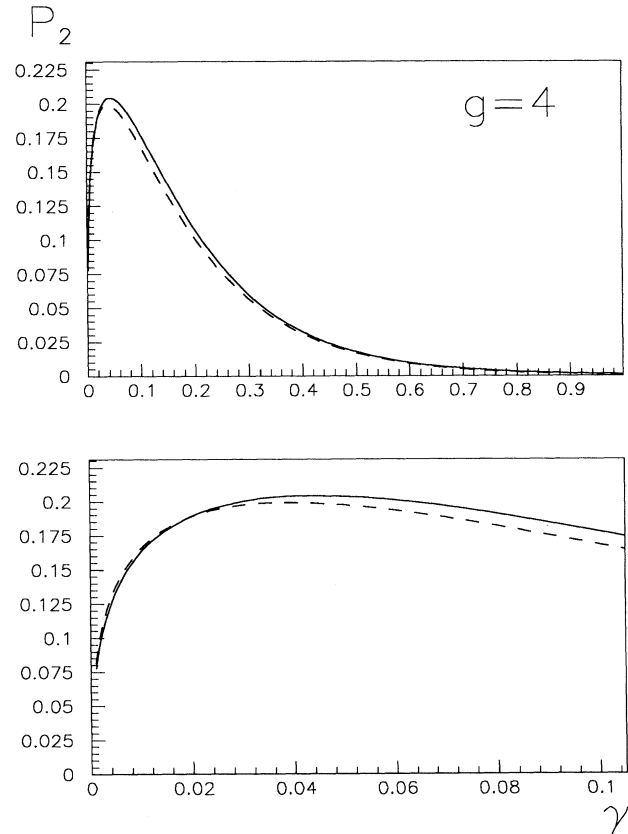
FIG. 16. The same as in Fig. 15, but at a potential barrier of $16k_B T$.

pect the P_n^M to be an accurate approximation in the case of $g \rightarrow \infty$ and $\gamma \rightarrow 0$. In any case, the behavior of the P_n^M shows more pronounced deviations from the exponential decay. The correct asymptotic slope for large n is never reproduced. The probabilities of very long jumps are overestimated by the analytical approximation; this fact is apparent in Fig. 9, where the less favorable case with respect to the validity of Eq. (3.22) is shown.

According to Eq. (3.22) and to the definition of w [see Eqs. (3.11) and (3.12)], the JLPD should be determined by the unique parameter Δ. In general this assumption is not correct; different couples of (γ, g) corresponding to the same Δ lead to different JLPD's. This is shown in Fig. 11, where we report the numerically calculated JLPD for two couples (γ, g) both corresponding to the same dissipation Δ: $\gamma = \frac{1}{10}$, $g = 4$ (black dots) and $\gamma = (\frac{2}{75})^{1/2}$, $g = \frac{3}{2}$ (squares). The asymptotic decay is clearly different and the case of lower friction and higher barrier shows more pronounced deviations from exponentiality, being in better agreement with the P_n^M of Fig. 10, which correspond to both couples (γ, g).

The best agreement between the P_n and the P_n^M is found in the case of short jumps. In Figs. 12–17 the behavior of the probabilities of single and double jumps is
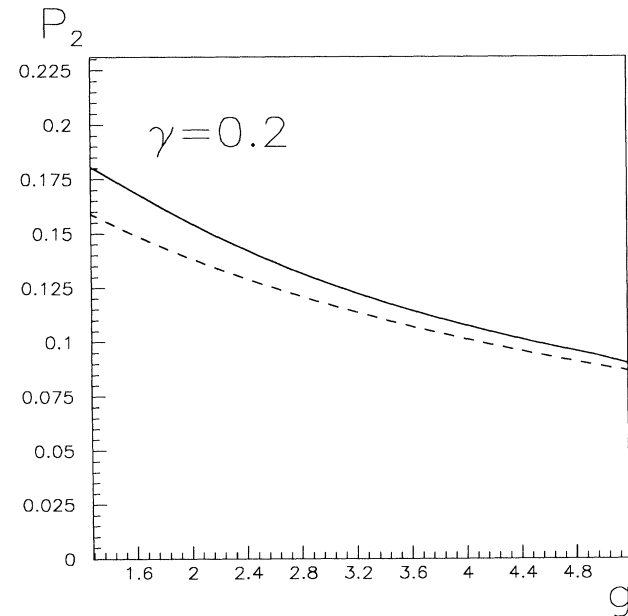

FIG. 17. Double-jump probability P_2 (full lines) as a function of g at a friction $\gamma = 0.2$. The dashed line is the analytical approximation P_2^M [see Eq. (3.22)].
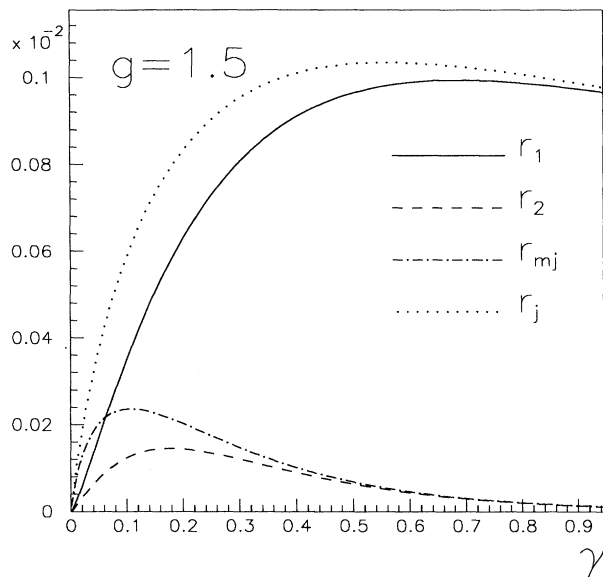
FIG. 18. Partial rates r_1 and r_2 [see Eq. (3.23)] and multiple-jump rate r_{mj} [see Eq. (3.24)] compared with the total jump rate r_j in the turnover region and below, at a barrier of $6k_BT$. All the quantities are numerically evaluated by solving the KKE.

shown as a function of the friction of two different values of the potential barrier (Figs. 12, 13 and 15, 16, respectively) and, at fixed friction, as a function of g (Figs. 14 and 17). In all those figures, P_1 and P_2 are represented by full lines, whereas P_1^M and P_2^M are represented by dashed lines. P_1 is an increasing function of both γ and g. Above the turnover P_1 quickly reaches its asymptotic
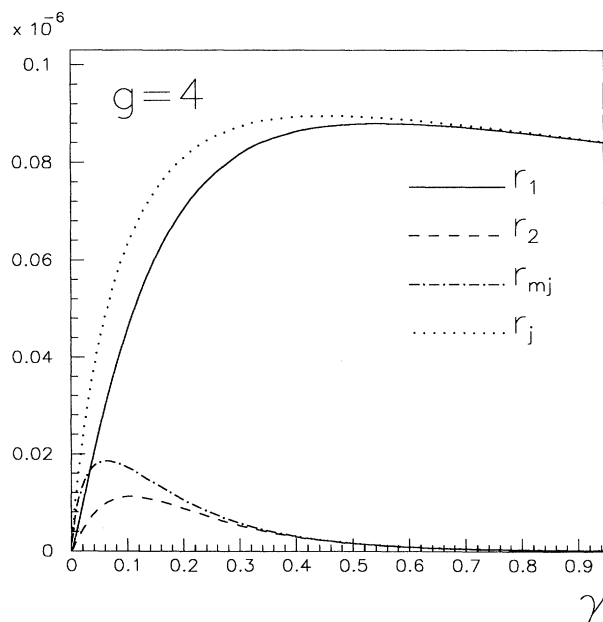

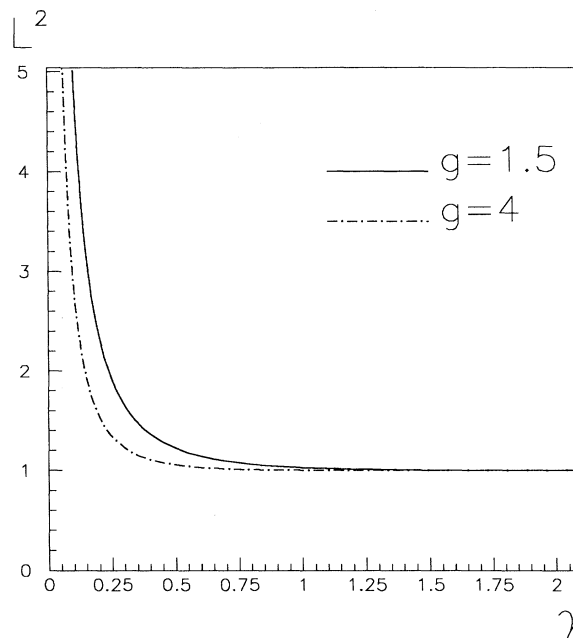FIG. 19. The same as in Fig. 18, but at a potential barrier of $16k_BT$.

FIG. 20. Mean-square jump length L^2 [see Eq. (3.25)] as a function of the friction for two values of the potential barrier.

value, which is of course 1. The analytical approximation overestimates P_1 in any case (at least in the parameter range explored by our numerical computations), being, however, in very good qualitative agreement with the numerical results even at $g \sim 1$; the quantitative agreement improves at high barriers. However, as it happens for the jump rate, the finite-barrier corrections are not negligible even at $E_a \sim 20k_BT$, especially in the underdamped regime.

The probability of double jumps tends to 0 both for $\gamma \to \infty$, where the multiple jumps become practically impossible, and for $\gamma \to 0$, where all the jump lengths tend to become equally probable. Thus P_2 must present a maximum, whose position is actually found well below the turnover: around $\gamma = 8 \times 10^{-2}$ at $g = 1.5$ and near $\gamma = 5 \times 10^{-2}$ at $g = 4$. The analytical approximation underestimates P_2 at high friction and overestimates it in the extremely underdamped regime; correspondingly the position of the maximum is shifted to lower γ values.

In Figs. 18 and 19 the partial rates r_n and the rate of multiple jumps r_{mj} are drawn, as numerically evaluated by the KKE. The partial rates are defined as

$$r_n = r_j P_n \, , \tag{3.23}$$

whereas r_{mj} is given by

$$r_{mj} = r_j(1 - P_1) \, . \tag{3.24}$$

All the partial rates present a maximum: the maximum of r_1 is to the right of the turnover, while the maxima of r_n, with $n \geq 2$, are located below the turnover, at smaller and smaller friction as n increases. Also r_{mj} presents a maximum at a friction below the turnover: around
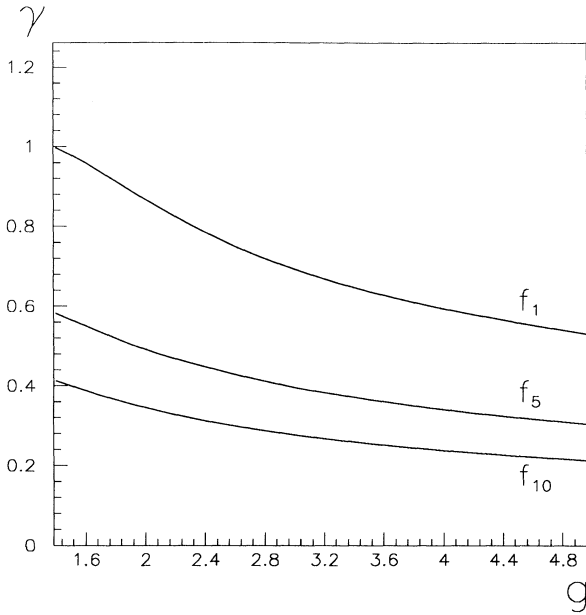
FIG. 21. Subdivision of the plane (g,γ) according to the probability of multiple jumps: $f_1(g)$ is the locus of the points for which the probability of multiple jumps is of 1%, whereas f_5 and f_{10} correspond to 5% and 10%, respectively.

$\gamma = 10^{-1}$ at $g = 1.5$ and $\gamma = 5 \times 10^{-2}$ at $g = 4$. The probability of multiple jumps increases towards 1 at vanishing friction, but the total rate vanishes in the same limit and therefore also the frequency of multiple jumps must vanish.

C. The multiple-jump regime

The importance of long jumps can be inferred from the mean-square jump length L^2,

$$L^2 = \sum_{n=1}^{\infty} n^2 P_n \ . \tag{3.25}$$

In the jump-diffusion regime, this quantity is related to the diffusion coefficient by Eq. (1.1) (notice that $\langle l^2 \rangle = a^2 L^2$) and it measures the mean-square number of unit cells covered by a jump. As results from Fig. 20, multiple jumps are almost completely negligible at $\gamma > 1$ even in the case of low barriers and become important in the turnover region. Below the turnover L^2 increases rapidly; in the limit $\gamma \to 0$, the diffusion coefficient diverges as γ^{-1} [2,35], the rate vanishes as γ, and therefore L^2 should diverge as γ^{-2}.

Finally in Fig. 21 the (g,γ) plane is divided in different regions according to the probability of multiple jumps. Of course, we consider the part of the parameter space where the jump-diffusion model can be safely applied [29], i.e., at sufficiently high barriers. The function $f_1(g)$ is defined as the locus of the points for which the probability of multiple jumps is of 1%, the functions $f_5(g)$ and $f_{10}(g)$ correspond to probabilities of 5% and 10%, respectively. Therefore, in the region above f_1 multiple

jumps are less probable then 1%; below f_{10} multiple jumps are more probable than 10%. Multiple jumps are always negligible at $\gamma > 1$, as predicted in the discussion of the mean-square jump length. The functions $f_1(g)$, $f_5(g)$, and $f_{10}(g)$ decrease approximately as $g^{-1/2}$; if the dissipation Δ was the unique parameter determining the JLPD, that behavior should be exact.

Finally, a comment on the normalization of the probabilities. The consistency of the method can be checked by verifying that the sum of the P_n is one. At high friction, where only single jumps are possible, there are some deviations from the normalization condition. These deviations are rather small even at $g = 1.5$ (the condition is fulfilled to 2 parts over 10^3) and decrease rapidly with the barrier (at $g = 4$ the deviation are of 2 parts over 10^7). Below the turnover region the probabilities are very well normalized even at low barriers ($g = 1.5$): to better than 10^{-6} at $\gamma = 0.1$ and better than 10^{-8} at $\gamma = 0.03$.

IV. CONCLUSIONS

In this paper we have presented an "exact" solution of the Kramers problem (really a jump-diffusion problem) in one-dimensional periodic potentials. Both the jump rate r_j and the JLPD have been obtained by a Fourier analysis of the decay function $f(q)$ of the discretized characteristic function $\Sigma_s^D(q,t)$; in the jump regime $f(q)$ practically coincides with the half-width of the quasielastic peak of the dynamic structure factor S_s. The theory is based on two ingredients: the separation of the in-cell motion from the jump dynamics among lattice sites and the numerical calculation of S_s by the MCFM. But what is the meaning of the word "exact" in this context? The jump rate itself is an asymptotic quantity, unambiguously defined only in the limit of a narrow and deep potential well ($g \to \infty$ for a cosine potential). Actually in the full range $g \geq 1.5$ (at least for a sinusoidal potential) the time scales of the problem are very well separated, the inverse rate being the longest. For a cosine potential, the relative difference between $f(q)$ and $\Delta\omega(q)/2$ in the first Brillouin zone is extremely small even at $g = 1$, being of the order of one part over 10^3; this difference decreases at least exponentially with increasing potential barrier. This fact indicates that the quasielastic peak of S_s is very well approximated, at least at $\omega \leq \Delta\omega(q)/2$ by a Lorentzian function [Eq. (2.14)]; the function $f(q)$ appearing in Eq. (2.14) is periodic over several Brillouin zones. Therefore the inelastic peak of S_s, centered at $\omega \simeq \omega_{\mathrm{osc}}$, does not influence the shape of the quasielastic peak at small ω. Below $g \simeq 1$ some inconsistency in the theory becomes evident: $f(q)$ differs from $\Delta\omega(q)$; the normalization of the JLPD is lost; the diffusion coefficient at very high friction [37,38], exactly known also at low barriers, is not reproduced by Eq. (1.1). In the spatial-diffusion regime, these difficulties can be removed, down to $g \simeq 0.6$, by taking into account the time of flight between nearest-neighbor cells [42]. However, at very low barriers, the continuous KKE dynamics cannot be approximated by any kind of discrete jump theory; the condition of local stability is lost and the in-cell dynamics cannot be separated from jump events. Thus we conclude that,

when it is possible to obtain an unambiguous definition of the rate, our solution is exact.

In this paper, the theory has been applied to a simple cosine potential with homogeneous friction. A wide range of frictions and potential barriers has been covered, the computational effort becoming really heavy only at $g > 5$ and $\gamma < 10^{-3}$.

Our numerical method does not contain free parameters [7], does not employ arbitrary bridging procedures in the turnover region [7,6], it is not an asymptotic result in the very high barrier limit [7,6,14], and it allows a quantitative determination of the finite-barrier corrections, whose importance has been recently recognized [12,19–21].

We have compared the numerical r_j and JLPD with analytical approximations of the Mel'nikov and Meshkov kind [9]; to our knowledge, this approach is the only one which has been extended to the periodic case [6]. The Hamiltonian approach [14], successfully tested in a recent paper [51] in the case of a metastable well, has not yet been extended to periodic potentials. In our case, the agreement between the numerical results and the analytical approximation is rather good, most of the differences being due to finite-barrier corrections (at least for r_j). It has been found that the corrections are particularly important in the underdamped regime.

The method of solution of the Kramers problem developed in this paper may be generalized in several directions. Of course, different shapes of the periodic po-

tential as well as position-dependent friction can be treated. Moreover, different kinetic equations, such as the linearized Boltzmann equation with BGK collision kernel [43], can be considered; the method may be applied also to the generalized Langevin equation with exponential memory friction [34].

Finally, we remark that low friction [24,31], small barriers [27], and position-dependent damping [25] may be of great interest in diffusion of atoms at crystal surfaces. In a recent molecular dynamics simulation of the motion of a single CO molecule adsorbed on Ni(111), Dobbs and Doren [31] found clear evidence of long (multiple) jumps. The authors estimated an energy barrier of $6k_BT$ ($g = 1.5$) and a velocity relaxation time corresponding to $\gamma \simeq 5 \times 10^{-2}$ at a temperature of 200 K. They extracted from the simulation the JLPD; the single-jump probability is smaller than 40% and the mean-square jump length is of about $10a^2$. They found that almost all jumps occur on straight lines; therefore a one-dimensional model for the JLPD may be meaningful. The KKE with cosine potential gives, at those g and γ, a mean-square jump length of the same order; however, the simulation does not show the typical KKE deviations from the exponential decay of the jump probabilities.

[1] *Noise in Nonlinear Systems,* edited by F. Moss and P. V. E. McClintock (Cambridge University Press, Cambridge, England, 1989).
[2] H. Risken, *The Fokker-Planck Equation* (Springer, Berlin, 1989), and references therein.
[3] N. G. Van Kampen, *Stochastic Processes in Physics and Chemistry* (North-Holland, Amsterdam, 1981).
[4] H. A. Kramers, Physica 7, 284 (1940).
[5] P. Hänngi, P. Talkner, and M. Borkovec, Rev. Mod. Phys. 62, 251 (1990), and references therein.
[6] V. I. Mel'nikov, Phys. Rep. 209, 1 (1991).
[7] M. Büttiker, E. P. Harris, and R. Landauer, Phys. Rev. B 28, 1268 (1983).
[8] B. Carmeli and A. Nitzan, Phys. Rev. Lett. 51, 233 (1983).
[9] V. I. Mel'nikov and S. V. Meshkov, J. Chem. Phys. 85, 1018 (1986).
[10] R. F. Grote and J. T. Hynes, J. Chem. Phys. 73, 2715 (1980); 77, 3736 (1982).
[11] P. Hänggi and F. Mojtabai, Phys. Rev. A 26, 1168 (1982).
[12] E. Pollak, S. C. Tucker, and B. J. Berne, Phys. Rev. Lett. 65, 1399 (1990).
[13] H. Grabert, Phys. Rev. Lett. 61, 1683 (1988).
[14] E. Pollak, H. Grabert, and P. Hänggi, J. Chem. Phys. 91, 4073 (1989).
[15] Surjit Singh, P. Krishnan, and G. W. Robinson, Phys. Rev. Lett. 68, 2608 (1992).
[16] P. Krishnan, Surjit Singh, and G. W. Robinson, Phys. Rev. A 45, 5408 (1992); J. Chem. Phys. 97, 5516 (1992).
[17] G. A. Voth, J. Chem. Phys. 97, 5908 (1992); J. B. Strauss, J. M. Gomez Llorente, and G. A. Voth, *ibid.* 98, 4082

(1993).
[18] A. M. Berezhkovskii, E. Pollak, and V. Yu. Zitserman, J. Chem. Phys. 97, 2422 (1992).
[19] P. Talkner and E. Pollak, Phys. Rev. E 47, 21 (1993).
[20] E. Pollak and P. Talkner, Phys. Rev. E 47, 922 (1993).
[21] V. I. Mel'nikov (unpublished).
[22] H. Risken and K. Voigtländer, J. Stat. Phys. 41, 825 (1985); K. Voigtländer and H. Risken, Chem. Phys. Lett. 105, 506 (1984).
[23] W. Dieterich, P. Fulde, and I. Peschel, Adv. Phys. 29, 527 (1980).
[24] R. Ferrando, R. Spadacini, and G. E. Tommei, Phys. Rev. B 45, 444 (1992).
[25] G. Wahnström, Surf. Sci. 159, 311 (1985); Phys. Rev. B 33, 1020 (1986); J. Chem. Phys. 84, 5931 (1986).
[26] S. C. Ying, Phys. Rev. B 41, 7068 (1990); T. Ala-Nissila and S. C. Ying, Prog. Surf. Sci. 39, 227 (1992).
[27] R. Ferrando, R. Spadacini, and G. E. Tommei, Surf. Sci. 251/252, 773 (1991).
[28] R. Ferrando, R. Spadacini, and G. E. Tommei, Phys. Rev. A 46, 699 (1992).
[29] R. Ferrando, R. Spadacini, G. E. Tommei, and G. Caratti, Physica A 195, 506 (1993); unfortunately, in this reference, the FWHM of the quasielastic peak $\Delta\omega(q)$ was called $f(q)$.
[30] G. Ehrlich, Surf. Sci. 246, 1 (1991); M. Lovisa and G. Ehrlich, J. Phys. (Paris) Colloq. 50, C8-279 (1989).
[31] K. D. Dobbs and D. J. Doren, J. Chem. Phys. 97, 3722 (1992).
[32] R. Ferrando, R. Spadacini, and G. E. Tommei, Physica A

196, 83 (1993).

[33] H. Risken and H. D. Vollmer, Z. Phys. B **33**, 297 (1979).

[34] A. Igarashi and T. Munakata, J. Phys. Soc. Jpn. **57**, 2439 (1988); A. Igarashi, N. G. Stocks, and P. V. E. McClintock, J. Stat. Phys. **66**, 1059 (1992).

[35] R. Ferrando, R. Spadacini, and G. E. Tommei, Surf. Sci. **265**, 273 (1992).

[36] R. Landauer, in *Noise in Nonlinear Systems,* edited by F. Moss and P. V. E. McClintock (Cambridge University Press, Cambridge, England, 1989), Vol. I, p. 1.

[37] S. Lifson and J. L. Jackson, J. Chem. Phys. **36**, 2410 (1962).

[38] R. Festa and E. G. D'Agliano, Physica A **90**, 229 (9178).

[39] R. Ferrando, R. Spadacini, G. E. Tommei, and A. C. Levi, Physica A **173**, 141 (1991).

[40] V. P. Zhdanov, Surf. Sci. **214**, 289 (1989).

[41] G. J. Moro and A. Polimeno, Chem. Phys. Lett. **189**, 133 (1992).

[42] R. Ferrando, R. Spadacini, and G. E. Tommei (unpublished).

[43] R. Ferrando, R. Spadacini, and G. E. Tommei, Chem. Phys. Lett. **202**, 248 (1993).

[44] C. T. Chudley and R. J. Elliott, Proc. Phys. Soc. London **77**, 353 (1961).

[45] R. Ferrando, R. Spadacini, and G. E. Tommei, Surf. Sci. **287/288**, 886 (1993).

[46] T. T. Tsong, Prog. Surf. Sci. **10**, 165 (1980).

[47] M. Büttiker and R. Landauer, Phys. Rev. Lett. **52**, 1250 (1984); Phys. Rev. B **30**, 1551 (1984).

[48] W. Dieterich, T. Geisel, and I. Peschel, Z. Phys. B **29**, 5 (1978).

[49] S. Glasstone, K. J. Laidler, and H. Eyring, *The Theory of Rate Processes* (McGraw-Hill, New York, 1941).

[50] R. Ferrando, R. Spadacini, and G. E. Tommei (unpublished).

[51] S. Linkwitz, H. Grabert, E. Turlot, D. Esteve, and M. H. Devoret, Phys. Rev. A **45**, 3369 (1992).